BASIC SCIENCE

Relevant Anatomic and Morphological Measurements of the Rat Spine

Considerations for Rodent Models of Human Spine Trauma

Nicolas V. Jaumard, PhD,* Jennifer Leung, BA,† Akhilesh J. Gokhale, MS,† Benjamin B. Guarino, BS,†
William C. Welch, MD,* and Beth A. Winkelstein, PhD*†

Study Design. Basic science study measuring anatomical features of the cervical and lumbar spine in rat with normalized comparison with the human.

Objective. The goal of this study is to comprehensively compare the rat and human cervical and lumbar spines to investigate whether the rat is an appropriate model for spine biomechanics investigations.

Summary of Background Data. Animal models have been used for a long time to investigate the effects of trauma, degenerative changes, and mechanical loading on the structure and function of the spine. Comparative studies have reported some mechanical properties and/or anatomical dimensions of the spine to be similar between various species. However, those studies are largely limited to the lumbar spine, and a comprehensive comparison of the rat and human spines is lacking.

Methods. Spines were harvested from male Holtzman rats (n = 5) and were scanned using micro– computed tomography and digitally rendered in 3 dimensions to quantify the spinal bony anatomy, including the lateral width and anteroposterior depth of the vertebra, vertebral body, and spinal canal, as well as the vertebral body and intervertebral disc heights. Normalized measurements of the vertebra, vertebral body, and spinal canal of the rat were computed and compared with corresponding measurements from the literature for the human in the cervical and lumbar spinal regions.

Results. The vertebral dimensions of the rat spine vary more between spinal levels than in humans. Rat vertebrae are more slender than human vertebrae, but the width-to-depth axial aspect ratios are very similar in both species in both the cervical and lumbar regions, especially for the spinal canal.

Conclusion. The similar spinal morphology in the axial plane between rats and humans supports using the rat spine as an appropriate surrogate for modeling axial and shear loading of the human spine.

Key words: cervical spine, lumbar spine, anatomy, vertebra, spine, spinal canal, human, rat, vertebral body, intervertebral disc.

Level of Evidence: N/A

Spine 2015;40:E1084–E1092

Animal models simulating spinal trauma and degenerative changes are used to define pathophysiological mechanisms and develop therapies for their treatment and/or prevention.[1–13] Few studies use bipeds,[14–16] whereas rat models are used commonly to study the mechanical and/or physiological responses of spinal tissues to loading.[17–24] Despite their popularity owing to their enabling high-throughput assessment and affordability, there are also differences that may limit the use of the rat model.

The spine in quadrupeds is loaded along its long axis during both standing and walking,[25,26] which is similar to the axial loading of the human spine by gravity. However, both the spine's range of motion and stiffness differ between humans and quadrupeds depending on the spinal level and the direction of motion/loading.[25,27] Disc height, cross-sectional area, and polar moment of inertia each have been used as normalizing parameters to study the anatomical and mechanical properties of isolated spinal components.[19,21] Although such normalization may be useful for comparing responses of the motion segment or disc in the axial plane, the 3-dimensional (3D) anatomy must be considered for scenarios involving the entire spine, or a spinal region, to mechanical loading in different planes and directions.

Indeed, the anatomy and geometry of the rat and human spines have been compared.[20,28] The normalized spinal canal is more elliptical in the neck of Sprague-Dawley rats than in humans, especially at the lowest cervical levels.[28] This anatomical difference was hypothesized as being due

to differences in the cervicothoracic lordosis or morphology of the spinal cord between rats and humans.[28] Lumbar discs have a similar geometry in both species when accounting for the axial dimensions of the disc, either by its cross-sectional area or height.[20] Although mammalian cadaveric vertebrae have been measured using calipers,[19,29] radiography, magnetic resonance imaging, and micro–computed tomography (CT), imaging techniques enable more accurate quantitative assessments.[28,30–32] Despite many studies establishing valuable comparisons of the anatomical and geometric features of the spine, as well as limited mechanical characteristics, for a wide range of species, work has focused only on the intervertebral disc and/or spinal canal dimensions.

The main objective of this study was to compare the anatomy of the rat and human cervical and lumbar spines to investigate potential anatomical rationale for using the rat as a proxy for the human spine in biomechanical investigations. Currently, there are limited anatomical investigations comparing the rat cervical spine with that of the biped human spine, despite an increasing number of biomechanical rat models focusing on the cervical spine.[18,33–43] In addition, axial spinal loading affects the disc, the facet joints, and the neural arches, as well as the vertebral bodies, and the geometry of *all* of these structures must be quantitatively evaluated to fully capture the spinal anatomy. The goals of this study were to measure several relevant dimensions of vertebral structures and to compute anatomical ratios for the rat cervical and lumbar spines to compare with values for the human spine in the literature. Whole rat spines were harvested and imaged using micro-CT for precise digital measurements of the vertebrae and intervertebral discs at the subaxial cervical and the lumbar levels and were compared against the corresponding human spinal dimensions.

MATERIALS AND METHODS

Five 12-week-old male Holtzman rats (Harlan Sprague-Dawley; Indianapolis, IN; 328 ± 19 g) were housed under US Department of Agriculture- and Association for Assessment and Accreditation of Laboratory Animal Care-compliant conditions with a 12- to 12-hour light-dark cycle and free access to food and water. All experimental procedures were approved by the Institutional Animal Care and Use Committee and carried out according to the guidelines of the Committee for Research and Ethical Issues of the International Association for the Study of Pain.[44]

The rat spine was harvested after transcardial perfusion with 200 mL phosphate-buffered saline, and fixed with 300 mL 4% paraformaldehyde. The spine was harvested *en bloc* from the C3 vertebra to the L5 vertebra, cleared of the paraspinal muscles, postfixed in 4% paraformaldehyde. The C1, C2, and L6 vertebrae were not harvested because of their unique anatomy in each species and a lack of correspondence with the human spine anatomy (namely L6). Metal beads (1 mm diameter) were glued to the spinous processes at C7, T1, L1, and L5 in order to label the cervical, thoracic, and lumbar regions. High-resolution images were acquired using micro-CT (vivaCT 40; Scanco Medical; Wayne, PA) in multislice mode; DICOM images were acquired at a slice thickness of 38 μm and a 1024 × 1024 axial field of view, with 32-bit-gray levels spanning each spinal region. Using the image analysis software, ITK-SNAP, individual vertebrae were identified and delineated with a semiautomatic segmentation process on the basis of the level-set method.[45] Adjacent slices with vertebral bone delineation were stacked together to generate a 3D rendering of each cervical and lumbar vertebrae and the entire spine (Figure 1).

The 3D reconstructed vertebrae were imported into the 3-Matic software (Materialise; Leuven, Belgium) to

Figure 1. Three-dimensional renderings of cervical and lumbar vertebrae of a young adult male Holtzman rat (not to scale to show features). Dimensions are indicated on the axial view of a cervical (C4) and lumbar vertebra (L3) and on the right anterolateral view of the cervical (left) and lumbar (right) spines. VBw indicates vertebral body width; VBd, vertebral body depth; Vw, vertebral length; SCw, spinal canal width; SCd, spinal canal depth; Vd, vertebral depth; VBh, vertebral body height; IVDh, intervertebral disc height.
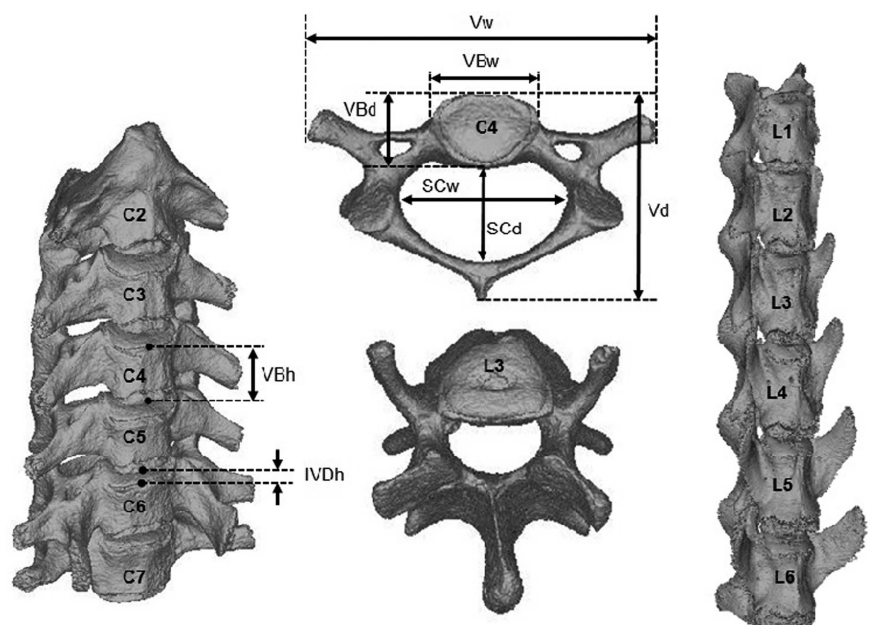
TABLE 1. Nomenclature Employed to Describe the Spinal Anatomy	
Acronym	**Description**
VBw	Maximum vertebral body length along the lateromedial direction.
VBd	Maximum vertebral body length along the anteroposterior direction.
VBh	Vertebral body length from the superior aspect of its upper endplate to the inferior aspect of its lower endplate measured at the anterior edge of each vertebra.
Vw	Maximum vertebra length along the lateromedial direction.
Vd	Maximum vertebra length along the anteroposterior direction.
SCw	Maximum lateral dimensions of spinal canal normal to midline.
SCd	Maximum spinal canal length along the anteroposterior direction.
IVDh	Intervertebral disc height from the inferior aspect of the corresponding upper endplate to the superior aspect of lower endplate.

quantitatively measure various features of the bony anatomy. Anatomical landmarks were identified on the axial and sagittal views of each rendered vertebra (Figure 1). Linear measurements were made using those points and with similar techniques as described previously for human and animal studies[28,29,46] (Table 1). Using the superior axial view, the anteroposterior and lateral dimensions of each vertebra (depth Vd; width Vw), vertebral body (depth VBd; width VBw), and spinal canal (depth SCd; width SCw) were measured (Figure 1; Table 1). The vertebral body height (VBh) and intervertebral disc height (IVDh) were measured on the anterior face of the vertebral bodies (Figure 1; Table 1). In addition, the vertebral body width and depth, as well as the spinal canal width and depth, were normalized by the vertebral depth and the vertebral width at each spinal level. The vertebral body height measurements were also normalized by the corresponding vertebral body depth. These anatomical ratios account for anatomical differences due to any variability in rat size and also enable comparison with the human spine anatomy.

All measurements were made 3 times by a single operator (A.J.G.) for each spinal level for each rat. Averages were computed for each dimension for each spinal level and for each rat and then averaged across all rats to calculate overall average measurements at each spinal level. Thirteen anatomical ratios describing the features of the vertebrae at each level were computed for the rats. Four ratios—vertebral width-to-depth (Vw/Vd), vertebral body width-to-depth (VBw/VBd), spinal canal width-to-depth (SCw/SCd), and vertebral body height-to-depth (VBh/VBd)—were used to characterize the ellipticity and slenderness of the rat spine. Those same anatomical dimensions of the human cervical and lumbar spines were calculated from the corresponding dimensions reported in the literature.[46–62] Ratios were compared between species
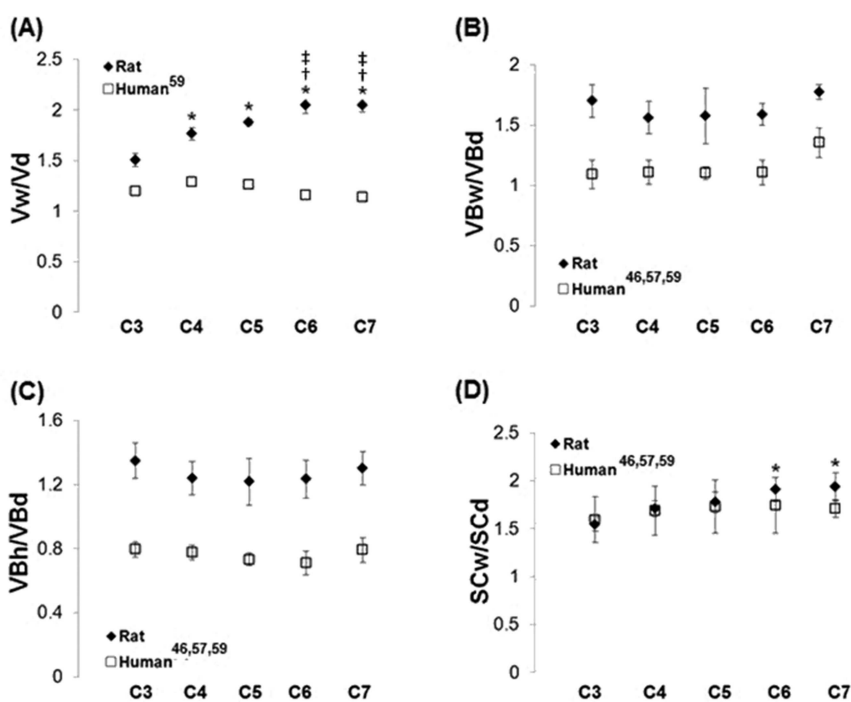
Figure 2. Comparison of the rat and human anatomical ratio of the cervical **(A)** Vw/Vd, **(B)** VBw/VBd, **(C)** VBh/VBd, and **(D)** SCw/SCd. Significant differences ($P < 0.05$) between vertebral levels in the rat are indicated relative to C3 (*), C4 (†), and C5 (‡). Vw/Vd indicates vertebral width-to-depth; VBw/VBd, vertebral body width-to-depth; VBh/VBd, vertebral body height-to-depth; SCw/SCd, spinal canal width-to-depth.

using a 2-way analysis of variance and a *post hoc* Tukey test, with species and vertebral level as factors.

RESULTS

Overall, the normalized anatomy of the cervical spine is similar across levels and between species, but there is less inter-level variation in the human than in the rat. Of the 13 computed ratios, only those describing the vertebral body (VBw/VBd and VBh/VBd) and Vw/Vd are significantly greater in rats than in humans. The cervical vertebral width-to-depth ratio (Vw/Vd) of the rat increases caudally from 1.50 ± 0.06 at C3 to 2.05 ± 0.07 at C7, which is significantly greater ($P \leq 0.0001$) than the corresponding range of values in the human (1.29 at C4; 1.14 at C7) (Figure 2A; Table 2). Vw/Vd values being greater than 1 indicate that the cervical vertebrae axial shape is elliptical in both species. However, the rat cervical vertebrae are 1.5 to 2 times wider than they are deep, whereas the cervical vertebrae in humans are about as wide as they are deep in the dorsal-ventral direction. This trend is similar in that rat cervical vertebral bodies are more elongated laterally (VBw/VBd) and more slender (VBh/VBd) than in humans (Figure 2B, C; Table 2). The rat cervical VBw/VBd ratio is significantly greater ($P < 0.03$) than the corresponding human ratio (1.09 ± 0.12 at C3 to 1.35 ± 0.12 at C7). But in both species, this ratio is similar across cervical levels (Figure 2B; Table 2). The same trend is evident across levels for the slenderness ratio (VBh/VBd), which is 60% to 74% greater ($P \leq 0.0001$) in rats than in humans (Figure 2C; Table 2). However, the ellipticity of the spinal canal (SCw/SCd) is similar between the 2 species (Figure 2D; Table 2).

The same similarities between levels and across species exist in the lumbar spine for anatomic ratios. All but 1 of the lumbar ratios are similar between species. The width-to-depth ratios of the lumbar vertebrae (Vw/Vd), vertebral bodies (VBw/VBd), and spinal canal (SCw/SCd) are similar overall in both species except at several isolated levels (Figure 3; Table 3). The vertebral ellipticity (Vw/Vd) is significantly greater ($P = 0.015$) in rats than in humans at L1, but it is close to 1 in both species at all other levels (Figure 3A; Table 3), indicating that the L2–L5 vertebrae are almost as wide as they are deep in both species. The ellipticity of the vertebral body (VBw/VBd) is similar in both species ($P = 0.4941$), ranging from 1.30 ± 0.08 to 1.56 ± 0.14 in rats and 1.35 ± 0.13 to 1.46 ± 0.05 in humans (Figure 3B, Table 3). In addition, the ellipticity of the spinal canal (SCw/SCd) is also

TABLE 2. Average ($\pm$SD) Cervical Anatomical Dimensions and Ratios for the Rat

	C3 or C2–C3	C4 or C3–C4	C5 or C4–C5	C6 or C5–C6	C7 or C6–C7
VBw	3.14 ± 0.17	3.01 ± 0.16	3.02 ± 0.33	3.05 ± 0.21	3.50 ± 0.10
VBd	1.85 ± 0.08	1.94 ± 0.11	1.92 ± 0.11	1.92 ± 0.07	1.97 ± 0.06
VBh	2.49 ± 0.19	2.40 ± 0.15	2.34 ± 0.19	2.36 ± 0.18	2.57 ± 0.19
Vw	9.03 ± 0.34	9.65 ± 0.38	9.98 ± 0.42	10.92 ± 0.37	11.10 ± 0.32
Vd	6.02 ± 0.40	5.48 ± 0.23	5.31 ± 0.19*	5.34 ± 0.21*	5.43 ± 0.19*
SCw	4.37 ± 0.08	4.63 ± 0.11	4.76 ± 0.08	4.99 ± 0.13	4.99 ± 0.14
SCd	2.83 ± 0.14	2.72 ± 0.12	2.69 ± 0.16	2.62 ± 0.13	2.58 ± 0.16
IVDh	N/A	0.80 ± 0.09	0.67 ± 0.05	0.50 ± 0.04	0.51 ± 0.05
Vw/Vd	1.50 ± 0.06	1.76 ± 0.06*	1.88 ± 0.03*	2.05 ± 0.08*†‡	2.05 ± 0.07*†‡
VBw/Vd	0.52 ± 0.03	0.55 ± 0.03	0.57 ± 0.05	0.57 ± 0.04	0.64 ± 0.02
VBd/Vd	0.31 ± 0.02	0.35 ± 0.01	0.36 ± 0.02	0.36 ± 0.01	0.36 ± 0.01
VBw/Vw	0.35 ± 0.02	0.31 ± 0.01	0.30 ± 0.03	0.28 ± 0.01	0.31 ± 0.01
VBd/Vw	0.20 ± 0.01	0.20 ± 0.01	0.19 ± 0.01	0.18 ± 0.00	0.18 ± 0.01
VBw/VBd	1.70 ± 0.13	1.56 ± 0.13	1.58 ± 0.23	1.59 ± 0.09	1.77 ± 0.06
VBh/VBd	1.35 ± 0.11	1.24 ± 0.10	1.22 ± 0.15	1.24 ± 0.12	1.30 ± 0.11
SCw/SCd	1.55 ± 0.07	1.71 ± 0.08	1.78 ± 0.11	1.91 ± 0.13*	1.94 ± 0.15*
SCw/Vw	0.48 ± 0.02	0.48 ± 0.01	0.48 ± 0.02	0.46 ± 0.01	0.45 ± 0.01
SCd/Vw	0.31± 0.02	0.28 ± 0.01	0.27 ± 0.01	0.24 ± 0.01	0.23 ± 0.02
SCw/Vd	0.73 ± 0.05	0.85 ± 0.03	0.90 ± 0.02	0.94 ± 0.05	0.92 ± 0.04
SCd/Vd	0.47 ± 0.02	0.50 ± 0.03	0.51 ± 0.02	0.49 ± 0.01	0.48 ± 0.02
IVDh/VBh	N/A	0.34 ± 0.06	0.29 ± 0.04	0.22 ± 0.03	0.21 ± 0.02

Significant differences ($P < 0.05$) between vertebral levels for the rat are indicated as C3 (*), C4 (†), and C5 (‡). Shaded cells indicate a significant difference ($P \leq 0.006$) between the rat and the human.

N/A indicates not applicable.

TABLE 3. Average (±SD) Lumbar Anatomical Dimensions and Ratios for the Rat				
	L1 or L1–L2	**L2 or L2–L3**	**L3 or L3–L4**	**L4 or L4–L5**	**L5 or L5–S1**
VBw	3.56 ± 0.08	3.57 ± 0.08	3.68 ± 0.16	3.70 ± 0.15	4.14 ± 0.23
VBd	2.30 ± 0.20	2.41 ± 0.10	2.54 ± 0.19	2.77 ± 0.12	3.19 ± 0.28
VBh	5.84 ± 0.45	6.53 ± 0.34	6.86 ± 0.34	6.87 ± 0.12	6.71 ± 0.22
Vw	8.08 ± 0.30	8.00 ± 0.35	8.11 ± 0.17	9.26 ± 0.83	10.71 ± 0.66
Vd	8.20 ± 0.29	8.38 ± 0.25	9.17 ± 0.54	9.70 ± 0.78	10.74 ± 0.73*†‡
SCw	3.85 ± 0.20	3.54 ± 0.22	3.24 ± 0.17	2.98 ± 0.21	2.57 ± 0.29
SCd	2.84 ± 0.29	2.39 ± 0.47	1.98 ± 0.30	1.55 ± 0.14	1.31 ± 0.15
IVDh	1.02 ± 0.23	1.13 ± 0.17	1.19 ± 0.26	1.31 ± 0.27	1.09 ± 0.07
Vw/Vd	0.98 ± 0.05	0.96 ± 0.02	0.87 ± 0.05	0.95 ± 0.03	0.99 ± 0.05
VBw/Vd	0.43 ± 0.02	0.43 ± 0.01	0.40 ± 0.01	0.38 ± 0.01	0.39 ± 0.02
VBd/Vd	0.28 ± 0.02	0.29 ± 0.01	0.28 ± 0.02	0.28 ± 0.02	0.30 ± 0.01
VBw/Vw	0.44 ± 0.02	0.45 ± 0.02	0.46 ± 0.02	0.40 ± 0.02	0.38 ± 0.01
VBd/Vw	0.29 ± 0.03	0.30 ± 0.01	0.31 ± 0.02	0.30 ± 0.02	0.29 ± 0.02
VBw/VBd	1.56 ± 0.14	1.48 ± 0.04	1.45 ± 0.05	1.34 ± 0.06	1.30 ± 0.08
VBh/VBd	2.56 ± 0.35	2.72 ± 0.20	2.71 ± 0.24	2.49 ± 0.13	2.12 ± 0.23*†‡
SCw/SCd	1.36 ± 0.12	1.52 ± 0.23	1.66 ± 0.18	1.94 ± 0.15*	1.97 ± 0.19*†
SCw/Vw	0.48 ± 0.02	0.44 ± 0.04	0.40 ± 0.02	0.32 ± 0.05	0.24 ± 0.05
SCd/Vw	0.35 ± 0.05	0.30 ± 0.07	0.25 ± 0.04	0.16 ± 0.02	0.12 ± 0.02
SCw/Vd	0.47 ± 0.03	0.42 ± 0.03	0.36 ± 0.03	0.31 ± 0.05	0.24 ± 0.04
SCd/Vd	0.35 ± 0.04	0.29 ± 0.06	0.22 ± 0.04	0.16 ± 0.01	0.12 ± 0.02
IVDh/VBh	0.18 ± 0.06	0.17 ± 0.03	0.17 ± 0.04	0.19 ± 0.04	0.17 ± 0.01

Significant differences ($P < 0.05$) between vertebral levels for the rat are indicated as L1 (*), L2 (†), and L3 (‡). Shaded cells indicate a significant difference ($P \leq 0.0155$) between the rat and the human.
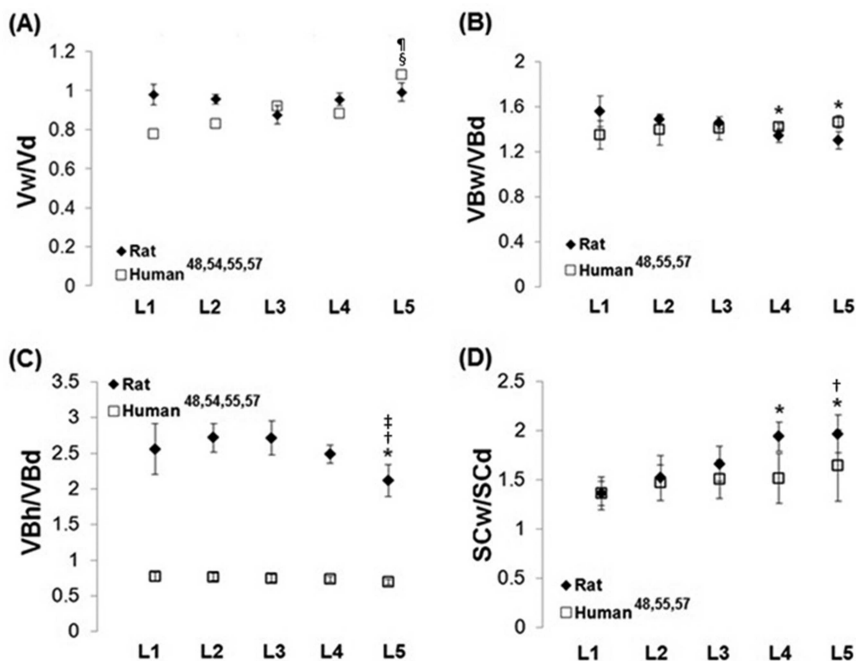

Figure 3. Comparison of the lumbar **(A)** Vw/Vd, **(B)** VBw/VBd, **(C)** VBh/VBd, and **(D)** SCw/SCd ratios between the rat and the human. Significant differences ($P < 0.05$) between levels in the rat are indicated relative to L1 (*), L2 (†), L3 (‡), and between levels in the human relative to L1 (§), L2 (¶). Vw/Vd indicates vertebral width-to-depth; VBw/VBd, vertebral body width-to-depth; VBh/VBd, vertebral body height-to-depth; SCw/SCd, spinal canal width-to-depth.

similar between the 2 species at all levels (Figure 3D; Table 3). In contrast, the slenderness of the vertebral body (VBh/VBd) is significantly greater ($P \leq 0.0001$) in rats (2.56 ± 0.35 at C3; 2.12 ± 0.23 at C7) than in humans (0.77 ± 0.06 at C3; 0.69 ± 0.04 at C7) (Figure 3C; Table 3).

The vertebral dimensions of the rat spine vary more between vertebral levels than they do in the human spine. In the cervical spine, the vertebral width (Vw) increases by 23 ± 4% from C3 to C7 (Table 2) but not significantly. The vertebral depth (Vd) is the same at all levels from C4 to C7 but is significantly greater ($P \leq 0.043$) at C3 than at C5, C6, and C7 (Figure 2; Table 2). Accordingly, the cervical Vw/Vd ratio is significantly greater ($P \leq 0.01$) at C6 and C7 than at C3–C5 (Figure 2A; Table 2). Although the SCw/SCd ratio increases with caudal location in the rat, the C6 and C7 values are only significantly greater ($P \leq 0.0471$) than the ratio at C3 (Figure 2D, Table 2).

In the rat lumbar spine, both the spinal canal width (SCw) and the depth (SCd) generally decrease moving caudally but that is not significant (Table 3). The lumbar vertebral depth (Vd) increases caudally and is significantly greater ($P \leq 0.043$) at L5 than at L1–L3 (Table 3). Correspondingly, several lumbar ratios decrease moving caudally, except SCw/SCd, which increases (Figure 3; Table 3). Although Vw/Vd is consistent across lumbar level (Figure 3A; Table 3), the vertebral body (VBh/VBd) is significantly ($P \leq 0.018$) more slender at L5 than at levels L1 through L3, which are similar to each other (Figure 3C; Table 3). The ellipticity of the vertebral body (VBw/VBd) is also significantly ($P < 0.015$) smaller at L4 and L5 than at L1 (Figure 3B; Table 3). In contrast, the spinal canal (SCw/SCd) is significantly more wide than it is deep at L4 and L5 than at L1 and L2 (Figure 3D; Table 3). Unlike the rat, these same ratios in the human remain mostly uniform across levels in the lumbar spine, except for the vertebral width-to-depth ratio (Vw/Vd), which is significantly ($P \leq 0.017$) greater at L5 than at L1 and L2 (Figure 3A).

DISCUSSION
Overall, the majority of the normalized dimensions in the cervical spine are generally similar between the rat and the human. Of the 13 anatomical ratios, only 3 in the cervical spine and 1 in the lumbar spine are larger in the rat than in the human (Figures 2A–C and 3C; Tables 2 and 3). Anatomical comparisons indicate that despite having more slender and elliptical vertebral bodies, the cervical and lumbar vertebrae of Holtzman rats generally have very similar shapes to the human ones. From a mechanical perspective, more slender vertebrae facilitate more flexibility in the spine, which is consistent with the sagittal and lateral mobility of the horizontally oriented head on the thorax in quadrupeds. The species differences in the cervical width-to-depth ratios (Vw/Vd, VBw/VBd) (Figure 2; Table 2) are likely also related to differences in the musculature and movement requirements for the head and neck motion between humans and rats.[63]

Differences in neck slenderness have been previously reported for studies investigating sex-based anatomical differences in the spine. Females have a thinner neck[64] and exhibit greater cervical range of motion in all directions.[65] Females also have a greater dynamic cervical segmental range of motion and a weaker and more slender neck than males, which may explain their being more prone to neck injuries than males.[64] Although males have taller C1–C5 vertebrae and a heavier head, which could lead to more susceptibility for neck injury, particularly in spinal bending, their vertebrae and vertebral bodies are also wider and deeper, and their muscles are stronger, providing greater protection against injurious cervical bending than for females.[64] The rat's cervical spine exhibits a similar anatomically based ability to resist injurious loading from bending. In quadrupeds, the cervical spine supports the head, acting as a cantilever beam that is hinged at the cervicothoracic junction. Because the aspect ratios of both the cervical vertebrae and the isolated vertebral bodies are larger in the rat, they likely provide greater cross-sectional area to mitigate bending stresses. This notion is further supported by the fact that the width of both the cervical vertebrae and the vertebral bodies is larger in the lower levels in the rat, with the greatest Vw/Vd and VBw/VBd at C7 (Table 2) where the bending moment is the greatest. However, these differences in the slenderness and ellipticity of the cervical spine between species have little effect for loading scenarios that do not involve bending and are limited to those directed axially or transverse to that direction.
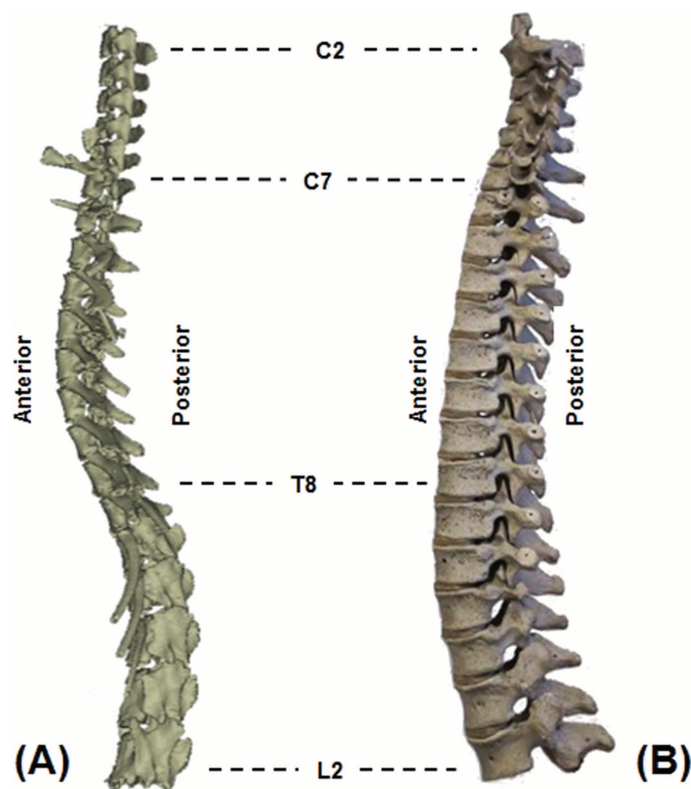

Figure 4. Lateral view of the **(A)** rat and **(B)** human spines showing the corresponding second (C2) and seventh (C7) cervical, 8 (T8) thoracic, and second (L2) lumbar vertebrae. Ventral is to the left and dorsal is to the right for both spines (not to scale).

Among all of the measurements, only the spinal canal width-to-depth ratio is similar at *all* levels in *both* spinal regions for *both* species (Figures 2D and 3D). Despite the rat having a more slender spine than the human (Figure 4), the similarity in the aspect ratio of the spinal canal between species suggests that canal dimensions can be scaled for biomechanical studies in the rodent. The dimensions of the vertebral body (VBw, VBd) and spinal canal (SCw, SCd) normalized by the overall vertebral width and depth are similar across levels in the rat as in the human (Tables 2 and 3). Finally, the average disc height (IVDh/VBh) in the cervical spine is equivalent in the rat (0.27 ± 0.07) and the human (0.36 ± 0.06). Collectively, these measurements further suggest *and support* that the cervical spine of the rat can serve as an appropriate surrogate for the human spine under axial load.

The spinal canal and vertebral body dimensions and disc height measured here are comparable with those reported for rodents of various strains and ages, obtained by direct measurements with a caliper and from 2D digital images.[19,20,28,31] However, those studies focused only on the spinal canal, the vertebral body, and/or the intervertebral disc in either the cervical or lumbar region. In our study, micro-CT and 3D rendering provide accurate quantification of vertebral dimensions in *both* spinal regions of the rat. Although our measurements vary slightly from those previously reported, that is likely due to differences in the measurement techniques and the animal size and strain. The similarity in spinal anatomy between rats aged 3 to 12 months supports the use of young Holtzman rats for comparison with humans.

Overall, anatomical differences and similarities between the rat spine and the human spine must be considered when interpreting findings in response to mechanical loading in animal models.[19] Because spine biomechanics are directly related to the global and local spinal anatomy, animals with normalized spinal dimensions similar to the human can serve as a mechanical analogue model.[20,28–30] The 3D anatomical dimensions of both the vertebrae and intervertebral discs in young male Holtzman rats were found to be very similar to the human in both the cervical and lumbar regions. Particularly, the similarities in the size in the axial plane between species in both spinal regions suggest that the mechanical responses of the spine to axial and shear loading can be considered equivalent across species. However, because the rat has a more slender spine than the human, it is likely not an appropriate model for biomechanical studies involving sagittal or lateral bending. This study evaluates only the geometry of spinal features and does not incorporate evaluation of factors such as bone density, age, or degenerative changes, all of which have been shown to vary in other animal models and to contribute to spinal responses—biomechanical or otherwise.[31,33,66,67] Moreover, variation in facet orientation and differences placed on the lumbar spine due to quadruped and biped differences also contribute to the spine's structure and function, although facet orientation was not addressed here. Nonetheless, as the complexity of studies in the rat continues to increase (as in many studies already published),[9,11,18,21,24,31,66–69] the detailed anatomic

descriptions like those provided here will provide important utility for calculating metrics of moments of inertia, stress calculations, and other relevant responses of the beams, like the spine.

Acknowledgments

➤ Key Points

- ❑ The anatomical dimensions of the cervical and lumbar spines vary more between vertebral levels in the rat than in the human.
- ❑ Because rats have a more slender spine than humans, the rat is not an appropriate model for biomechanical studies involving sagittal or lateral bending.
- ❑ Similar normalized spinal morphology in the axial plane between the 2 species makes the rat spine an appropriate surrogate for modeling axial and shear loading of the human spine.

References

1. Damle SR, Rawlins BA, Boachie-Adjei O, et al. Lumbar spine intervertebral disc gene delivery: a pilot study in Lewis rats. *HSS J* 2013;9:36–41.
2. Dudli S, John Ferguson S, Haschtmann D. Severity and pattern of posttraumatic intervertebral disc degeneration depends on the type of injury. *Spine J* 2014;14:1256–64.
3. Gales N, Kunz SN, Rocksén D, et al. Muscle pathologies after cervical spine distortion-like exposure—a porcine model. *Traffic Inj Prev* 2013;14:828–34.
4. Gregory DE, Bae WC, Sah RL, et al. Disc degeneration reduces the delamination strength of the anulus fibrosis in the rabbit anular disc puncture model. *Spine J* 2014;14:1265–71.
5. Humadi A, Freeman BJ, Moore RJ, et al. A comparison of radiostereometric analysis and computed tomography for the assessment of lumbar spinal fusion in a sheep model. *Evid Based Spine Care J* 2013;4:78–89.
6. Kiely PD, Brecevich AT, Taher F, et al. Evaluation of a new formulation of demineralized bone matrix putty in a rabbit posterolateral spinal fusion model. *Spine J* 2014;14:2155–63.
7. Lee JH, Ryu HS, Seo JH, et al. Negative effect of rapidly resorbing properties of bioactive glass-ceramics as bone graft substitute in a rabbit lumbar fusion model. *Clin Orthop Surg* 2014;6:87–95.
8. Lu Y, Chen C, Kallakuri S, et al. Development of an in vivo method to investigate biomechanical and neurophysiological properties of spine facet joint capsules. *Eur Spine J* 2005;14:565–72.
9. Martin JT, Milby AH, Chiaro JA, et al. Translation of an engineered nanofibrous disc-like angle-ply structure for intervertebral disc replacement in a small animal model. *Acta Biomater* 2014;10:2473–81.
10. Ohtori S, Inoue G, Miyagi M, et al. Pathomechanisms of discogenic low back pain in humans and animal models. *Spine J* 2015;15:1347–55.
11. Qin J, He X, Wang D, et al. Artificial cervical vertebra and intervertebral complex replacement through the anterior approach in animal model: a biomechanical and in vivo evaluation of a successful goat model. *PLoS One* 2012;7:e52910.

12. Roberto R, Dezfuli B, Deuel C, et al. A biomechanical comparison of three spondylolysis repair techniques in a calf spine model. *Orthop Traumatol Surg Res* 2013;99:66–71.

13. Yilgor C, Demirkiran HG, Aritan S, et al. Fusionless instrumentation in growing spine and adjacent segment problems: an experimental study in immature pigs. *Spine* 2013;38:2156–64.

14. Elias PZ, Nuckley DJ, Ching RP. Effect of loading rate on the compressive mechanics of the immature baboon cervical spine. *J Biomech Eng* 2006;128:18–23.

15. Hernandez CJ, Loomis DA, Cotter MM, et al. Biomechanical allometry in hominoid thoracic vertebrae. *J Hum Evol* 2009;56:462–70.

16. Ledet EH, Sachs BL, Brunski JB, et al. Real-time in vivo loading in the lumbar spine: part 1. Interbody implant: load cell design and preliminary results. *Spine* 2000;25:2595–600.

17. Antunes E, Oliveira P, Oliveira MJ, et al. Histomorphometric evaluation of the coronary artery vessels in rats submitted to industrial noise. *Acta Cardiol* 2013;68:285–9.

18. Baig HA, Guarino BB, Lipschutz D, et al. Whole body vibration induces forepaw and hind paw behavioral sensitivity in the rat. *J Orthop Res* 2013;31:1739–44.

19. Beckstein JC, Sen S, Schaer TP, et al. Comparison of animal discs used in disc research to human lumbar disc: axial compression mechanics and glycosaminoglycan content. *Spine* 2008;33:E166–73.

20. O'Connell GD, Vresilovic EJ, Elliott DM. Comparison of animals used in disc research to human lumbar disc geometry. *Spine* 2007;32:328–33.

21. Showalter BL, Beckstein JC, Martin JT, et al. Comparison of animal discs used in disc research to human lumbar disc: torsion mechanics and collagen content. *Spine* 2012;37:E900–7.

22. Talac R, Friedman JA, Moore MJ, et al. Animal models of spinal cord injury for evaluation of tissue engineering treatment strategies. *Biomaterials* 2004;25:1505–10.

23. Winkelstein BA. How can animal models inform on the transition to chronic symptoms in whiplash? *Spine* 2011;36:S218–25.

24. Wirth F, Schempf G, Stein G, et al. Whole-body vibration improves functional recovery in spinal cord injured rats. *J Neurotrauma* 2013;30:453–68.

25. Kandziora F, Pflugmacher R, Scholz M, et al. Comparison between sheep and human cervical spines: an anatomic, radiographic, bone mineral density, and biomechanical study. *Spine* 2001;26:1028–37.

26. Smit TH. The use of a quadruped as an in vivo model for the study of the spine—biomechanical considerations. *Eur Spine J* 2002;11:137–44.

27. Busscher I, van der Veen AJ, van Dieën JH, et al. In vitro biomechanical characteristics of the spine: a comparison between human and porcine spinal segments. *Spine* 2010;35:E35–42.

28. Flynn JR, Bolton PS. Measurement of the vertebral canal dimensions of the neck of the rat with a comparison to the human. *Anat Rec* 2007;290:893–9.

29. Boszczyk BM, Boszczyk AA, Putz R. Comparative and functional anatomy of the mammalian lumbar spine. *Anat Rec* 2001;264:157–68.

30. Frobin W, Leivseth G, Biggemann M, et al. Vertebral height, disc height, posteroanterior displacement and dens-atlas gap in the cervical spine: precision measurement protocol and normal data. *Clin Biomech* 2002;17:423–31.

31. Laing AC, Cox R, Tetzlaff W, et al. Effects of advanced age on the morphometry and degenerative state of the cervical spine in a rat model. *Anat Rec* 2011;294:1326–36.

32. Wilke HJ, Kettler A, Wenger KH, et al. Anatomy of the sheep spine and its comparison to the human spine. *Anat Rec* 1997;247:542–55.

33. Ding Y, Jiang J, Zhou J, et al. The effects of osteoporosis and disc degeneration on vertebral cartilage endplate lesions in rats. *Eur Spine J* 2014;23:1848–55.

34. Gerardo-Nava J, Mayorenko II, Grehl T, et al. Differential pattern of neuroprotection in lumbar, cervical and thoracic spinal cord segments in an organotypic rat model of glutamate-induced excitotoxicity. *J Chem Neuroanat* 2013;53:11–7.

35. Griffin C, Choong WY, Teh W, et al. Head and cervical spine posture in behaving rats: Implications for modeling human conditions involving the head and cervical spine. *Anat Rec* 2015;298:455–62; doi: 10.1002/ar.23049.

36. Karadimas SK, Moon ES, Yu WR, et al. A novel experimental model of cervical spondylotic myelopathy (CSM) to facilitate translational research. *Neurobiol Dis* 2013;54:43–58.

37. Kartha S, Zeeman ME, Baig HA, et al. Upregulation of BDNF and NGF in cervical intervertebral discs exposed to painful whole-body vibration. *Spine* 2014;39:1542–8.

38. Kras JV, Tanaka K, Gilliland TM, et al. An anatomical and immunohistochemical characterization of afferents innervating the C6/C7 facet joint after painful joint loading in the rat. *Spine* 2013;38:E325–31.

39. Nicholson KJ, Zhang S, Gilliland TM, et al. Riluzole effects on behavioral sensitivity and the development of axonal damage and spinal modifications that occur after painful nerve root compression. *J Neurosurg Spine* 2014;20:751–62.

40. Moon ES, Karadimas SK, Yu WR, et al. Riluzole attenuates neuropathic pain and enhances functional recovery in a rodent model of cervical spondylotic myelopathy. *Neurobiol Dis* 2014;62:394–406.

41. Syré PP, Weisshaar CL, Winkelstein BA. Sustained neuronal hyperexcitability is evident in the thalamus after a transient cervical radicular injury. *Spine* 2014;39:E870–7.

42. Wang L, Jiang Y, Lao J, et al. Contralateral C7 transfer to lower trunk via the prespinal route in the repair of brachial plexus injury: an experimental study in rats. *J Plast Reconstr Aesthet Surg* 2014;67:1282–7.

43. Weishaupt N, Vavrek R, Fouad K. Training following unilateral cervical spinal cord injury in rats affects the contralesional forelimb. *Neurosci Lett* 2013;539:77–81.

44. Zimmermann M. Ethical guidelines for investigations of experimental pain in conscious animals. *Pain* 1983;16:109–10.

45. Ferrari V, Parchi P, Condino S, et al. An optimal design for patient-specific templates for pedicle spine screws placement. *Int J Med Robot* 2013;9:298–304.

46. Panjabi MM, Duranceau J, Goel V, et al. Cervical human vertebrae. Quantitative three-dimensional anatomy of the middle and lower regions. *Spine* 1991;16:861–9.

47. Andersson GB, Schultz A, Nathan A, et al. Roentgenographic measurement of lumbar intervertebral disc height. *Spine* 1981;6:154–8.

48. Berry JL, Moran JM, Berg WS, et al. A morphometric study of human lumbar and selected thoracic vertebrae. *Spine* 1987;12:362–7.

49. Dabbs VM, Dabbs LG. Correlation between disc height narrowing and low-back pain. *Spine* 1990;15:1366–9.

50. Francis CC. Dimensions of the cervical vertebrae. *Anat Rec* 1955;122:603–9.

51. Frobin W, Brinckmann P, Biggemann M, et al. Precision measurement of disc height, vertebral height and sagittal plane displacement from lateral radiographic views of the lumbar spine. *Clin Biomech* 1997;12:S1–63.

52. Hurxthal LM. Measurement of anterior vertebral compressions and biconcave vertebrae. *Am J Roentgenol Radium Ther Nucl Med* 1968;103:635–44.

53. Kutoglu T, Kilincer C, Hamamcioglu MK, et al. The agreement between radiographic and surgical measurements of intervertebral disc height: a cadaveric study. *Trakya Univ Tip Fak Derg* 2010;27:385–90.

54. Nissan M, Gilad I. The cervical and lumbar vertebrae—an anthropometric model. *Eng Med* 1984;13:111–4.

55. Panjabi MM, Goel V, Oxland T, et al. Human lumbar vertebrae. Quantitative three-dimensional anatomy. *Spine* 1992;17:299–306.

56. Robin S, Skalli W, Lavaste F. Influence of geometrical factors on the behavior of lumbar spine segments: a finite element analysis. *Eur Spine J* 1994;3:84–90.

57. Tan SH, Teo EC, Chua HC. Quantitative three-dimensional anatomy of cervical, thoracic and lumbar vertebrae of Chinese Singaporeans. *Eur Spine J* 2004;13:137–46.

58. Tibrewal SB, Pearcy MJ. Lumbar intervertebral disc heights in normal subjects and patients with disc herniation. *Spine* 1985;10:452–4.

59. Tominaga T, Dickman CA, Sonntag VK, et al. Comparative anatomy of the baboon and the human cervical spine. *Spine* 1995;20:131–7.

60. Tosun O, Fidan F, Erdil F, et al. Assessment of lumbar vertebrae morphology by magnetic resonance imaging in osteoporosis. *Skeletal Radiol* 2012;41:1583–90.

61. Videman T, Battié MC, Gibbons LE, et al. Aging changes in lumbar discs and vertebrae and their interaction: a 15-year follow-up study. *Spine J* 2014;14:469–78.

62. Zhou SH, McCarthy ID, McGregor AH, et al. Geometrical dimensions of the lower lumbar vertebrae—analysis of data from digitised CT images. *Eur Spine J* 2000;9:242–8.

63. Graf W, de Waele C, Vidal PP, et al. The orientation of the cervical vertebral column in unrestrained awake animals. II. Movement strategies. *Brain Behav Evol* 1995;45:209–31.

64. Stemper BD, Yoganandan N, Pintar FA, et al. Anatomical gender differences in cervical vertebrae of size-matched volunteers. *Spine* 2008;33:E44–9.

65. Ferrario VF, Sforza C, Serrao G, et al. Active range of motion of the head and cervical spine: a three-dimensional investigation in healthy young adults. *J Orthop Res* 2002;20:122–9.

66. Gruber HE, Phillips R, Ingram JA, et al. Spontaneous age-related cervical disc degeneration in the sand rat. *Clin Orthop Relat Res* 2014;472:1936–42.

67. Robinson ST, Svet MT, Kanim LA, et al. Four-point bending as a method for quantitatively evaluating spinal arthrodesis in a rat model. *Comp Med* 2015;65:56–50.

68. Cunningham ME, Beach JM, Bilgic S, et al. In vivo and in vitro analysis of rat lumbar spine mechanics. *Clin Orthop Relat Res* 2010;468:2695–703.

69. Shahrokni M, Zhu Q, Liu J, et al. Design and biomechanical evaluation of a rodent spinal fixation device. *Spinal Cord* 2012;50:543–7.